ARTICULATED HUMAN MOTION TRACKING WITH HPSO

Vijay John, Spela Ivekovic
School of Computing, University of Dundee, Dundee, United Kingdom
vijayjohn@computing.dundee.ac.uk, spelaivekovic@computing.dundee.ac.uk

Emanuele Trucco
School of Computing, University of Dundee, Dundee, United Kingdom
manueltrucco@computing.dundee.ac.uk

Keywords: Articulated Human Motion Tracking, Hierarchical Particle Swarm Optimisation, Annealed Particle Filter

Abstract: In this paper, we address full-body articulated human motion tracking from multi-view video sequences acquired in a studio environment. The tracking is formulated as a multi-dimensional nonlinear optimisation and solved using particle swarm optimisation (PSO), a swarm-intelligence algorithm which has gained popularity in recent years due to its ability to solve difficult nonlinear optimisation problems. Our tracking approach is designed to address the limits of particle filtering approaches: it initialises automatically, removes the need for a sequence-specific motion model and recovers from temporary tracking divergence through the use of a powerful hierarchical search algorithm (HPSO). We quantitatively compare the performance of HPSO with that of the particle filter (PF) and annealed particle filter (APF). Our test results, obtained using the framework proposed by (Balan et al., 2005) to compare articulated body tracking algorithms, show that HPSO's pose estimation accuracy and consistency is better than PF and compares favourably with the APF, outperforming it in sequences with sudden and fast motion.

1 INTRODUCTION

Tracking articulated human motion from video sequences is an important problem in computer vision with applications in virtual character animation, medical posture analysis, surveillance, human-computer interaction and others. In this paper, we formulate the full-body articulated tracking as a nonlinear optimisation problem which we solve using particle swarm optimization (PSO), a recent swarm intelligence algorithm with growing popularity (Poli, 2007; Poli et al., 2008).

Because the full-body articulated pose estimation is a high-dimensional optimisation problem, we formulate it as a hierarchical PSO algorithm (HPSO) which exploits the inherent hierarchy of the human-body kinematic model, thus reducing the computational complexity of the search.

HPSO is designed to address the limits of the particle filtering approaches. Firstly, it removes the need for a sequence-specific motion model: the same algorithm with unmodified parameter settings is able to track different motions without any prior knowledge of the motion's nature. Secondly, it addresses the problem of divergence, a characteristic behaviour of particle filter implementations, whereby the filter loses track after a wrongly estimated pose and is unable to recover unless interactively corrected by the user or assisted by additional, higher-level motion models (Caillette et al., 2008). In contrast, our tracking approach is able to automatically recover from an incorrect pose estimate and continue tracking. Last but not least, in line with its ability to recover from an incorrect pose estimate, our HPSO tracker also initialises automatically on the first frame of the sequence, requiring no manual intervention.

This paper is organised as follows. We describe the related work in Section 2. Section 3 presents the PSO algorithm. In Section 4 we describe the body model and cost function used in our tracking approach and in Section 5 present the HPSO algorithm. We show the experimental results including a comparison of our algorithm with the particle filter (PF) and the annealed particle filter (APF) in Section 6. Section 7 contains conclusions and ideas for future work.

2 RELATED WORK

The approaches to articulated motion analysis can generally be divided into *generative* and *discriminative* methods. The generative methods use the *analysis-by-synthesis* approach, where the candidate pose is represented by an explicit body model and the appropriate likelihood function is evaluated to determine its fitness. The discriminative methods, on the other hand, represent the articulated pose implicitly by learning the mapping between the pose space and a set of image features. Combinations of both approaches have also been reported.

Our method fits under the umbrella of generative analysis-by-synthesis and we review the related work accordingly. We do not attempt to provide an exhaustive list of related research and instead refer the reader to one of the many recent surveys on this topic (Poppe, 2007).

As articulated pose estimation is a high-dimensional search problem, particle filtering approaches, with their ability to use non-linear motion models and explore the search space with a number of different hypotheses, have become very popular. An early attempt was the Condensation algorithm (Isard and Blake, 1998), which in its original form quickly became computationally unfeasible when applied to high-dimensional problem of articulated tracking (Deutscher and Reid, 2005).

Efforts to reduce the computational complexity and the required number of particles resulted in various extensions, some focusing on ways of partitioning the search space or modifying the sampling process (MacCormick and Isard, 2000; Sminchisescu and Triggs, 2003; Husz et al., 2007) and others advocating trained prior models (Vondrak et al., 2008; Caillette et al., 2008).

In our work, we also formulate the pose estimation as a hierarchical search problem, thereby partitioning the search space to reduce the computational complexity of the search, however, instead of using a particle filter to estimate the pose, we employ a powerful swarm intelligence global search algorithm, called particle swarm optimisation (PSO) (Kennedy and Eberhart, 1995). Similarly to the annealed particle filter (APF) and its genetic crossover extension (Deutscher and Reid, 2005), the idea is to allow the particles to explore the search space for a number of iterations per frame. The advantage of our method lies in the way the particles communicate with each other to find the optimum. Our method does not use any motion priors and we are able to demonstrate experimentally that our approach outperforms the APF with crossover operator by (Deutscher and Reid, 2005).

PSO is a swarm intelligence search technique which has been growing in popularity and has in the past 13 years been used to solve various non-linear optimisation problems in a number of areas, including computer vision (Poli, 2007). A recent publication by (Zhang et al., 2008) demonstrated an application of a variant of PSO, called sequential PSO, to box tracking in video sequences and theoretically demonstrated that their framework in essence represented a multi-layer importance sampling based particle filter. Applications of PSO to articulated pose estimation from multi-view still images have also been reported (Ivekovic and Trucco, 2006; Ivekovic et al., 2008), as well as articulated tracking from stereo data (Robertson et al., 2005; Robertson and Trucco, 2006).

The work reported in this paper is an extension of (Ivekovic and Trucco, 2006; Ivekovic et al., 2008) to full-body pose estimation from multi-view video sequences.

3 PARTICLE SWARM OPTIMISATION

Particle swarm optimisation (PSO) is a swarm intelligence technique introduced by (Kennedy and Eberhart, 1995). The idea originated from the simulation of a simplified social model, where the agents were thought of as collision-proof birds and the original intent was to graphically simulate the unpredictable choreography of a bird flock in their search for food. The original PSO algorithm was later modified by several researchers to improve its search capabilities and convergence properties. In this paper we use the PSO algorithm with an inertia weight parameter, introduced by (Shi and Eberhart, 1998).

3.1 PSO Algorithm with Inertia Weight Parameter

Assume an n-dimensional search space $\mathbb{S} \subseteq \mathbb{R}^n$, a swarm consisting of N particles, each particle representing a candidate solution to the search problem, and a cost function $f : \mathbb{S} \rightarrow \mathbb{R}$ defined on the search space. The i-th particle is represented as an n-dimensional vector $\mathbf{x}^i = (x_1, x_2, ..., x_n)^T \in \mathbb{S}$. The velocity of this particle is also an n-dimensional vector $\mathbf{v}^i = (v_1, v_2, ..., v_n)^T \in \mathbb{S}$. The best position encountered by the i-th particle so far (*personal* best) is denoted by $\mathbf{p}^i = (p_1, p_2, ..., p_n)^T \in \mathbb{S}$ and the value of the cost function at that position $pbest^i = f(\mathbf{p}^i)$. The index of the particle with the overall best position so far (*global* best) is denoted by g and $gbest = f(\mathbf{p}^g)$. The PSO algorithm can then be stated as follows:

1. **Initialisation**:

- Initialise a population of particles $\{\mathbf{x}^i\}, i = 1 \ldots N$, with random positions and velocities in the search space $\mathbb{S}$. For each particle evaluate the desired cost function f and set $pbest^i = f(\mathbf{x}^i)$. Identify the best particle in the swarm and store its index as g and its position as $\mathbf{p}^g$.

2. **Repeat** until the stopping criterion is fulfilled:

   - Move the swarm by updating the position of every particle $\mathbf{x}^i$, $i = 1 \ldots N$, according to the following two equations:

$$\begin{aligned} \mathbf{v}_{t+1}^i &= w\mathbf{v}_t^i + \varphi_1(\mathbf{p}_t^i - \mathbf{x}_t^i) + \varphi_2(\mathbf{p}_t^g - \mathbf{x}_t^i) \\ \mathbf{x}_{t+1}^i &= \mathbf{x}_t^i + \mathbf{v}_{t+1}^i \end{aligned} \quad (1)$$

     where subscript t denotes the time step (iteration).

   - For $i = 1 \ldots N$ update $\mathbf{p}^i$, $pbest^i$, $\mathbf{p}^g$ and $gbest$.

The stopping criterion is usually either the maximum number of iterations or the minimum gbest improvement. The parameters $\varphi_1 = c_1 rand_1()$ and $\varphi_2 = c_2 rand_2()$, where c is a constant and $rand()$ is a random number drawn from $[0,1]$, influence the *social* and *cognition* components of the swarm behaviour, respectively. In line with (Kennedy and Eberhart, 1995), we set $c_1 = c_2 = 2$, which gives the stochastic factor a mean of 1.0 and causes the particles to "overfly" the target about half of the time, while also giving equal importance to both social and cognition components. Parameter w is the inertia weight which we describe in more detail next.

3.2 Inertia weight parameter

The inertia weight w can remain constant throughout the search or change with time. It plays an important role in directing the exploratory behaviour of the particles: higher inertia values push the particles to explore more of the search space and emphasise their individual velocity, while lower inertia values force particles to focus on a smaller search area and move towards the best solution found so far.

In this paper, we use a time-varying inertia weight.We model the change over time with an exponential function which allows us to use a constant sampling step while gradually guiding the swarm from a global to more local exploration:

$$w(c) = \frac{A}{e^c}, \quad c \in [0, \ln(10A)], \quad (2)$$

where A denotes the starting value of w when the sampling variable $c = 0$ and c is incremented by $\Delta c = ln(10A)/C$, where C is the desired number of inertia weight changes. The optimisation terminates when $w(c)$ falls below 0.1.

4 BODY MODEL AND COST FUNCTION

In this section, we present a short summary of the body model and the cost function proposed by (Balan et al., 2005), which we adopt in our implementation. We adopt this framework to ensure a fair comparison with other body tracking algorithms reported.

4.1 Body model

The human body shape is modelled as a collection of truncated cones (Figure 1(a)). The underlying articulated motion is modelled with a kinematic tree containing 13 nodes, each node corresponding to a specific body joint. For illustration, the indexed joints are shown overlaid on the test subject in Figure 1(b). Every node can have up to 3 rotational DOF, while the root node also has 3 translational DOF. In total, we use 31 parameters to describe the full body pose (Table 1).

Table 1: Joints and their DOF

JOINT (index)	#	DOF
Global body position (1)	3	r_x, r_y, r_z
Global body orientation (1)	3	$\alpha_x^1, \beta_y^1, \gamma_z^1$
Torso orientation (2)	2	β_y^2, γ_z^2
Left clavicle orientation (3)	2	α_x^3, β_y^3
Left shoulder orientation (4)	3	$\alpha_x^4, \beta_y^4, \gamma_z^4$
Left elbow orientation (5)	1	β_y^5
Right clavicle orientation (6)	2	α_x^6, β_y^6
Right shoulder orientation (7)	3	$\alpha_x^7, \beta_y^7, \gamma_z^7$
Right elbow orientation (8)	1	β_y^8
Head orientation (9)	3	$\alpha_x^9, \beta_y^9, \gamma_z^9$
Left hip orientation (10)	3	$\alpha_x^{10}, \beta_y^{10}, \gamma_z^{10}$
Left knee orientation (11)	1	β_y^{11}
Right hip orientation (12)	3	$\alpha_x^{12}, \beta_y^{12}, \gamma_z^{12}$
Right knee orientation (13)	1	β_y^{13}
TOTAL	31	

4.2 Cost function

The cost function measures how well a candidate body pose matches the pose of the person in the video sequence. It consists of two parts, an edge-based part and a silhouette-based part.

In the edge-based part, a binary edge map is obtained by thresholding the image gradients. This map is then convolved with a Gaussian kernel to create a edge distance map, which determines the proximity of a pixel to an edge. The model points along the edge of the truncated cones are projected onto the edge map

and the mean square error (MSE) between the projected points and the edges in the map is computed.

In the silhouette-based part, a silhouette is obtained from the input images by statistical background subtraction with a Gaussian mixture model. A predefined number of points on the surface of the 3-D body model is then projected into the silhouette image and the MSE between the projected points and the silhouette computed.

Finally, the MSEs of the edge-based part and silhouette-based part are combined to give the cost function value $f(\mathbf{x}^i)$ of the i-th particle :

$$f(\mathbf{x}^i) = MSE^i_{edge} + MSE^i_{silhouette} \quad (3)$$

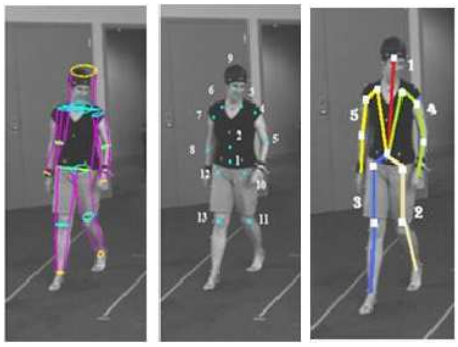

(a) (b) (c)

Figure 1: (a) The truncated-cone body model. (b) Joint positions. (c) Kinematic tree.

5 HPSO Algorithm

The work presented in this paper is an extension of (Ivekovic and Trucco, 2006; Ivekovic et al., 2008) where a PSO-based hierarchical framework is used to estimate the articulated upper-body pose with multi-view still images. This work extends the approach to tracking the full-body pose in multi-view video sequences. The tracking algorithm consists of three main components: the initialisation, the hierarchical pose estimation and the next-frame propagation, which we describe next.

5.1 Initialisation

The initialisation is fully automatic. Each particle in the swarm is assigned a random 31-dimensional position in the search space. A particle's position represents a possible body pose configuration, with the position vector specified as:

$$\mathbf{x}_i = (r_x, r_y, r_z, \alpha_x^1, \beta_y^1, \gamma_z^1, ..., \alpha_x^K, \beta_y^K, \gamma_z^K), \quad (4)$$

where r_x, r_y, r_z denote the position of the entire body (root of the kinematic tree) in the world coordinate system, and $\alpha_x^k, \beta_y^k, \gamma_z^k$, $k = 1 \ldots K$, refer to rotational degrees of freedom of joint k around the x, y, and z-axis, respectively, where $K+1$ is the total number of joints in the kinematic tree. Each particle is also assigned a random 31-dimensional velocity vector, giving it an exploratory direction in the search space.

5.2 Hierarchial Pose estimation

PSO has been successfully applied to various non-linear optimisation problems (Poli, 2007; Poli et al., 2008). However, as pointed out by (Robertson and Trucco, 2006; Ivekovic and Trucco, 2006), it becomes computationally prohibitive with increasing numbers of optimised DOF.

In order to make the implementation computationally feasible, we solve the pose estimation in a hierarchical manner, where the kinematic tree modelling the articulated motion is estimated in several stages, starting at the root and proceeding downwards towards the leaves. This is possible because the kinematic structure of the human body contains an inherent hierarchy in which the joints lower down the kinematic tree (e.g., elbows) are constrained by the joints higher up the tree (e.g., shoulders).

We use this property to subdivide the search space into several subspaces containing only a subset of DOF each, thus reducing the search complexity. The hierarchy of the kinematic structure starts with the position and orientation of the entire body in the world coordinate system. Changing either of these affects the configuration of every joint in the model. The kinematic tree then branches out into 5 chains: one for the neck and head, two for left and right arm, and two for left and right leg. The chains modelling the upper body form a subtree with the torso orientation as the root node. From the root node they then branch out independently.

The 5 branches of the kinematic tree are shown overlaid on the test subject in Figure 1(c). We split the search space into 12 different subspaces and correspondingly perform the hierarchical optimisation in 12 steps, detailed in Table 2. The subspaces are chosen so that only one limb segment at a time is optimised.

5.3 Next-Frame Propagation

Once the pose in a particular frame has been estimated, the particle swarm for the next frame is initialised by sampling the individual particle positions from a Gaussian distribution centred on the position of the best particle from the previous frame, with the

Table 2: Hierarchy of optimisation.

(Step 1) Global body pos.: 3DOF: r_x, r_y, r_z	**(Step 5)** Left lower arm orient.: 2DOF: γ_z^4, β_y^5	**(Step 9)** Left upper leg orient.: 2DOF: $\alpha_x^{10}, \beta_y^{10}$
(Step 2) Global body orient.: 3DOF: $\alpha_x^1, \beta_y^1, \gamma_z^1$	**(Step 6)** Right upper arm orient.: 4DOF: $\alpha_x^6, \beta_y^6, \alpha_x^7, \beta_y^7$	**(Step 10)** Left lower leg orient.: 2DOF: $\gamma_z^{10}, \beta_y^{11}$
(Step 3) Torso orient.: 2DOF: β_y^2, γ_z^2	**(Step 7)** Right lower arm orient.: 2DOF: γ_z^7, β_y^8	**(Step 11)** Right upper leg orient.: 2DOF: $\alpha_x^{12}, \beta_y^{12}$
(Step 4) Left upper arm orient.: 4DOF: $\alpha_x^3, \beta_y^3, \alpha_x^4, \beta_y^4$	**(Step 8)** Head orient.: 3DOF: $\alpha_x^9, \beta_y^9, \gamma_z^9$	**(Step 12)** Right lower leg orient.: 2DOF: $\gamma_z^{12}, \beta_y^{13}$

covariance set to a low value, in our case 0.01, to promote temporal consistency.

6 EXPERIMENTAL RESULTS

(Balan et al., 2005) published a Matlab implementation of an articulated full-body tracking evaluation software, which includes an implementation of PF and APF. This provided us with a platform to quantitatively evaluate our tracking algorithm. We implemented our tracking approach within their framework by substituting the particle filter code with our HPSO algorithm. All other parts of their implementation were kept the same to ensure a fair comparison.

Datasets: In our experiments, we used 4 datasets: the *Lee walk* sequence included in the Brown University evaluation software and 3 datasets courtesy of the University of Surrey: *Jon walk*, *Tony kick* and *Tony punch* sequences. The *Lee walk* dataset was captured with 4 synchronised grayscale cameras with resolution 640×480 at 60 fps and came with the ground truth articulated motion data acquired by a Vicon system, allowing for a quantitative comparison of the tracking results. The Surrey sequences were acquired by 10 synchronised colour cameras with resolution 720×576 at 25 fps.

HPSO setup: HPSO was run with only 10 particles and without any hard prior. The PSO parameters (inertia weight model, stopping condition) and the covariance of the Gaussian distribution used for propagating the swarm into the next frame were kept the same across all the datasets to demonstrate the versatility of our algorithm. The starting inertia weight was kept at 2 and the stopping inertia was fixed at 0.1 for all the sequences and this amounted to 60 PSO iterations per step in the hierarchical optimisation or 7200 likelihood evaluations per frame (12 steps per frame).

PF/APF setup: (Balan et al., 2005) use a zero-velocity motion model, where the noise drawn from a Gaussian distribution is equal to the maximum inter-frame difference and different for each dataset. Unlike the original APF algorithm (Deutscher and Reid, 2005), the Brown software uses a motion-capture-trained hard prior for the *Lee walk* sequence to initialise the tracking and eliminate particles with implausible poses. This significantly improves the accuracy of the APF tracking algorithm as seen in (Balan et al., 2005) and also confirmed by our experiments. Since we wanted to compare our algorithm with the original APF algorithm by (Deutscher and Reid, 2005), we ran our tests without the hard prior, except for initialisation which otherwise failed, as described later.

Testbed choice: To select the appropriate comparison testbed for PF, APF and HPSO, we ran two tests. In the first one, all three algorithms were set up to use the same number of likelihood evaluations to find the solution. In the second one, all three were given the same computation time. The setup was normalised to HPSO which required 7200 evaluations and took 70 seconds per frame. We therefore ran the PF with 7200 particles and the APF with 1440 particles and 5 annealing layers in the first experiment (Setup A), and PF with 3000 particles and APF with 600 particles and 5 annealing layers in the second experiment (Setup B).

The results of the first experiment showed that the same number of likelihood evaluations increased the temporal complexity of APF and PF to thrice that of PSO. Our results (Table 3), show that the tracking accuracy does not increase significantly with the increased number of particles. This result is parallel to the results observed in (Husz et al., 2007), where increasing the particle numbers beyond 500 does not result in any additional improvement. When comparing on the basis of temporal complexity, HPSO also outperformed both PF and APF (Table 3). Due to the high temporal complexity of PF and APF associated with Setup A, we decided to perform the rest of the experiments based on the Setup B.

Lee Walk Results: The results obtained at 60 fps (Figure 2) show that the performance of HPSO is comparable to that of APF and better than that of PF. Table 4 shows the error calculated as the distance

Table 3: MAP error in mm for the *LeeWalk* sequence with varying number of likelihood evaluations

Algorithm	testbed	MAP error
PF	(Setup A)	70.0 ± 21.2
APF	(Setup A)	68.38 ± 17.5
PF	(Setup B)	72 ± 20.5
APF	(Setup B)	68.83 ± 25
HPSO	(Setup A,B)	46.5 ± 8.48mm

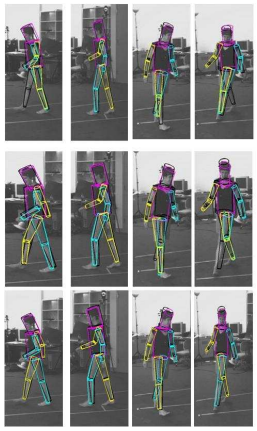

Figure 2: The results for the 60 fps Lee walk sequence for frames 1, 40, 80 and 120 with PF, APF and HPSO results in the 1st, 2nd and 3rd row, respectively.

between the ground-truth joint values and the values from the pose estimated in each frame, averaged over 5 trials. We also performed a comparison with a temporally subsampled Lee walk sequence by downsampling to 30 fps to increase the inter-frame motion. The distance error tabulated in Table 4 shows that the HPSO performs better than both the APF and the PF at the reduced frame rate. The graph comparing the distance-error for 30 fps sequences is shown in Figure 3. Results show that the accuracy of HPSO is not significantly affected by faster motion, while the performance of the APF and PF deteriorates.

Surrey sequence results: The Surrey test sequences contained faster motion than the Lee walk sequence. For rapid and sudden motion in the punch and kick sequence, HPSO performed better than APF and PF (Figure 7,6). Since we do not have the ground truth data for the Surrey dataset, we could not compute numerical errors as in the case of the *Lee walk* sequence. Instead, we chose to measure the overlap of the model's silhouette in the estimated pose with the image silhouettes and edges by modifying our cost function. The estimated pose measure O_n for the n-th

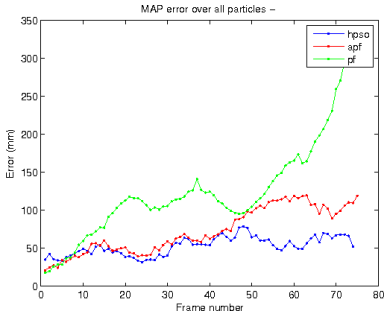

Figure 3: The distance error graph for 30 fps.

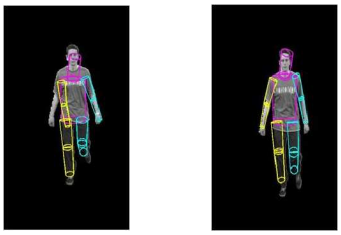

(a) Frame 28 (b) Frame 29

Figure 5: (a) an incorrect HPSO estimate due to error propagation (b) the estimate is corrected in the next frame.

frame is given as:

$$O_n = OvrLap^n_{edge} + OvrLap^n_{silhouette} \qquad (5)$$

The average overlap and standard deviation for a given sequence over 5 trials are shown in Table 5.

Recovery: Our experiments also confirmed that HPSO has the ability to recover from a wrong estimate, unlike PF and APF, where the error after a wrong estimate normally increases (the problem of *divergence*). E.g., in Figure 5, the right elbow is wrongly estimated by APF and is never recovered. This behaviour is even more pronounced in the PF. HPSO, on the other hand, recovers and finds the correct estimate in the following frame, in spite of wrongly estimating it in the previous frame (Figure 5).

Automatic initialisation: HPSO can initialise automatically on the first frame of the sequence. We tested the automatic initialisation on all 4 test sequences. A canonical initial pose (Figure 4(a,e)) was given as a starting point. The HPSO algorithm, initialised by sampling from a random distribution centered at the canonical pose, consistently found the correct position and orientation of the person in the initial frame, while PF and APF failed to find a better estimate due to the given starting point being too far from the solution.

Table 4: The distance error calculated for the Lee Walk sequences

Sequence	PF Mean ± Std.dev	APF Mean ± Std.dev	HPSO Mean ± Std.dev
LeeWalk60Hz	72± 20.55mm	68.38 ± 25mm	46.5±8.48mm
Leewalk30Hz	125.5± 56.7mm	72.6±29.9mm	52.5±11.7mm

Table 5: The silhouette/edge overlap measure for the Surrey sequence. Bigger number means better performance.

Sequence	PF Mean ± Std.dev	APF Mean ± Std.dev	HPSO Mean ± Std.dev
Jon Walk	1.311±0.027	1.350±0.025	1.3853±0.015
Tony Kick	1.108±0.095	1.197±0.041	1.2968±0.024
Tony Punch	1.253±0.018	1.26±0.01	1.3296±0.0117

7 CONCLUSIONS AND FUTURE WORK

We presented a hierarchical PSO algorithm (HPSO) for full-body articulated tracking, and demonstrated that it performs better than APF and PF, most notably in sequences with fast and sudden motion. HPSO also successfully addresses the problem of particle filter divergence through its search strategy and particle interaction and reduces drastically the need for a sequence-specific motion model.

An inherent limitation of algorithms with a weak motion model, is the dependence of its accuracy on the observation. In case of noisy silhouettes or missing body parts the accuracy would decrease. Another limitation that became evident during the experimental work, was error propagation: due to the hierarchical and sequential structure of the HPSO algorithm, an incorrect estimate higher up in the kinematic chain infuenced the accuracy of all the subsequent hierarchical steps. Although undesired, the error propagation was not fatal for the performance of the HPSO tracker, as it was still able to recover from a bad estimate in the subsequent frames (Figure 5).In our future work, we will address the error propagation problem as well as incorporate a better next frame strategy to further increase the accuracy and decrease the time complexity of the search.

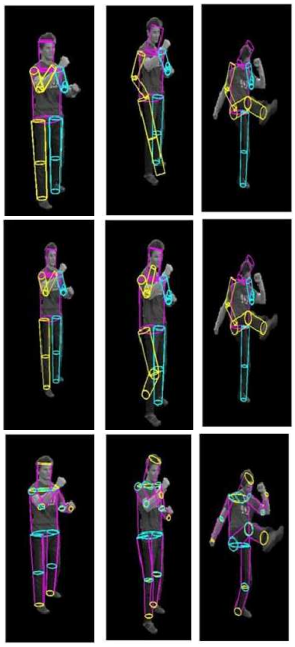

Figure 6: Results of Tony kick sequence illustrated for frames 1, 15 and 25. The PF, APF and HPSO results are displayed in the first, second and third row respectively.

ACKNOWLEDGEMENTS

This work is supported by EPSRC grant EP/080053/1 Vision-Based Animation of People in collaboration with Prof. Adrian Hilton at the University of Surrey (UK). We refer the readers to (Starck and Hilton, 2007) for further information on the Surrey test sequences.

REFERENCES

Balan, A. O., Sigal, L., and Black, M. J. (2005). A quantitative evaluation of video-based 3d person tracking. In *ICCCN '05: Proceedings of the 14th International Conference on Computer Communications and Networks*, pages 349–356. IEEE Computer Society.

Caillette, F., Galata, A., and Howard, T. (2008). Real-time 3-d human body tracking using learnt models of behaviour. *Computer Vision and Image Understanding*, 109(2):112–125.

Deutscher, J. and Reid, I. (2005). Articulated body motion capture by stochastic search. *International Journal of Computer Vision*, 61(2):185–205.

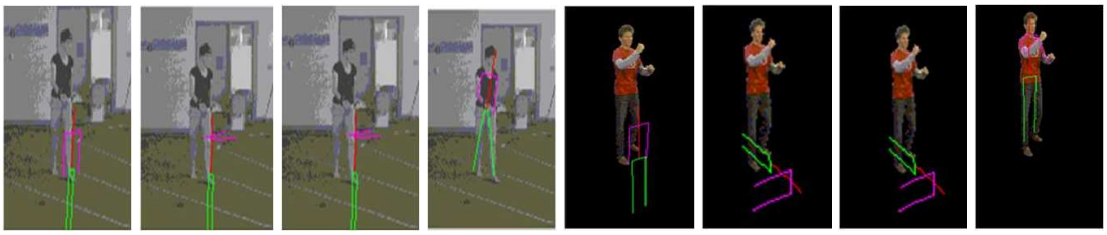

(a) (b) (c) (d) (e) (f) (g) (h)

Figure 4: The automatic initialisation results for the Lee walk (left) and Tony Kick (right) sequence. (a,e) The canonical initial pose for all three algorithms. (b,f) Unsuccessful PF and (c,g) unsuccessful APF initialisation. (d,h) successful HPSO initialisation.

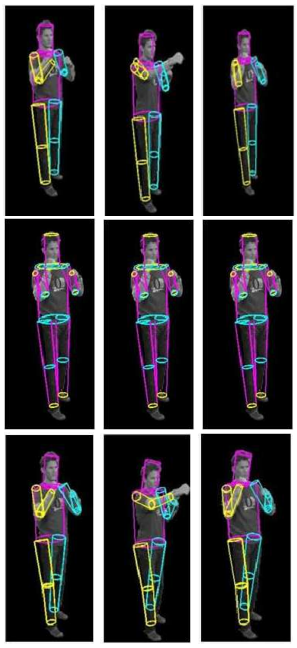

Figure 7: Results of Tony punch sequence, illustrated for frames 1, 15 and 25. The PF, APF and HPSO results are displayed in the first, second and third row respectively.

Husz, Z., Wallace, A., and Green, P. (2007). Evaluation of a hierarchical partitioned particle filter with action primitives. In *CVPR 2nd Workshop on Evaluation of Articulated Human Motion and Pose Estimation*.

Isard, M. and Blake, A. (1998). CONDENSATION - conditional density propagation for visual tracking. *International Journal of Computer Vision*, 29(1):5–28.

Ivekovic, S. and Trucco, E. (2006). Human body pose estimation with pso. In *Proceedings of IEEE Congress on Evolutionary Computation (CEC '06)*, pages 1256–1263.

Ivekovic, S., Trucco, E., and Petillot, Y. (2008). Human body pose estimation with particle swarm optimisation. *Evolutionary Computation*, 16(4).

Kennedy, J. and Eberhart, R. (1995). Particle swarm optimization. In *Proceedings of the IEEE International Conference on Neural Networks*, volume 4, pages 1942–1948.

MacCormick, J. and Isard, M. (2000). Partitioned sampling, articulated objects, and interface-quality hand tracking. In *Proceedings of the European Conference on Computer Vision (ECCV'00) - volume 2*, number 1843 in Lecture Notes in Computer Science, pages 3–19, Dublin, Ireland.

Poli, R. (2007). An analysis of publications on particle swarm optimisation applications. Technical Report CSM-649, University of Essex, Department of Computer Science.

Poli, R., Kennedy, J., Blackwell, T., and Freitas, A. (2008). Editorial for particle swarms: The second decade. *Journal of Artificial Evolution and Applications*, 1(1):1–3.

Poppe, R. (2007). Vision-based human motion analysis: An overview. *Computer Vision and Image Understanding (CVIU)*, 108(1-2):4–18.

Robertson, C. and Trucco, E. (2006). Human body posture via hierarchical evolutionary optimization. In *In: BMVC06. III:999*.

Robertson, C., Trucco, E., and Ivekovic, S. (2005). Dynamic body posture tracking using evolutionary optimisation. *Electronics Letters*, 41:1370–1371.

Shi, Y. H. and Eberhart, R. C. (1998). A modified particle swarm optimizer. In *Proceedings of the IEEE International Conference on Evolutionary Computation*, pages 69 – 73.

Sminchisescu, C. and Triggs, B. (2003). Estimating articulated human motion with covariance scaled sampling. *International Journal of Robotic Research*, 22(6):371–392.

Starck, J. and Hilton, A. (2007). Surface capture for performance based animation. *IEEE Computer Graphics and Applications*, 27(3):21–31.

Vondrak, M., Sigal, L., and Jenkins, O. C. (2008). Physical simulation for probabilistic motion tracking. In *Proceedings of CVPR 2008*, pages 1–8.

Zhang, X., Hu, W., Maybank, S., Li, X., and Zhu, M. (2008). Sequential particle swarm optimization for visual tracking. In *Proceedings of CVPR 2008*.